HYDROLOGICAL PROCESSES
Hydrol. Process. **20**, 3709–3724 (2006)
Published online in Wiley InterScience
(www.interscience.wiley.com) DOI: 10.1002/hyp.6384

Energy and water vapour exchanges over a mixedwood boreal forest in Ontario, Canada

M. R. Pejam,[1] M. A. Arain[1]* and J. H. McCaughey[2]

[1] *School of Geography and Earth Sciences, McMaster University, Hamilton, Ontario, L8S 4K1, Canada*
[2] *Department of Geography, Queen's University, Kingston, Ontario, K7L 3N6, Canada*

Abstract:

Measurements of energy, carbon dioxide and water vapour fluxes and supporting meteorological variables were made from 1 September 2003 to 31 August 2004 in a 74-year-old mixedwood forest in northern Ontario, Canada, using the eddy covariance technique. Land surface cover data analysis showed that although this forest is comprised of deciduous and coniferous species, their proportion throughout the forest was almost equal, resulting in a homogeneously mixedwood stand. The seasonal pattern of albedo showed a distinct pattern as a result of mixed deciduous and coniferous species with the first low radiation reflection period in early spring (between snowmelt and deciduous leaf-out), and the second low reflection period in late autumn (between senescence and snowfall). Root zone soil water content remained above 0·32 throughout the growing season, which is characteristic of wet soil conditions. The evaporative flux exceeded the sensible heat flux during most of the growing season. Daily mean evapotranspiration values during the peak growing season were about 2–2·5 mm day^{-1} with maximum values reaching up to 4–5 mm day^{-1} on sunny days. The total water loss over the 12-month measurement period was 480 ± 30 mm, while the total precipitation was 835 mm. Despite high soil water content, bulk surface conductance calculated using the inverted Penman–Monteith formulation, showed a strong correlation with vapour pressure deficit (VPD), indicating stomatal control on water loss during the afternoons with high atmospheric demand and during occasional dry periods. Bulk surface conductance values in this mixedwood forest were relatively higher than those in other boreal coniferous forests and were more similar to values observed in the southern boreal deciduous forests. The Priestley–Taylor α values showed a wide range but during most of the growing season its values were close to unity, indicating that water stress does not play a major role in the overall water loss from this boreal forest ecosystem, while energy supply has a strong control on evapotranspiration. These results will help parameterize accurately energy and water exchanges for the moist mixedwood forests in land surface-atmosphere interaction and hydrologic models. Copyright © 2006 John Wiley & Sons, Ltd.

KEY WORDS mixedwood boreal forest; evaporation; latent heat flux; energy fluxes; surface conductance; albedo; Priestley–Taylor α; eddy covariance

Received 1 August 2005; Accepted 12 April 2006

INTRODUCTION

The boreal forest is a vast ecosystem that encircles the northern hemisphere. It covers nearly one-fifth of the earth's vegetated land surface (Blanken *et al*., 1997; Baldocchi *et al*., 2000), and more than one-third of the Canadian landscape. Mixedwood forests that have both coniferous and deciduous species growing side by side are the dominant forest type in the central and eastern boreal regions of Canada. The differences in coniferous and deciduous species composition, phenology and physiology in mixedwood forests significantly influence the dynamics of energy, carbon dioxide and water vapour exchanges in these forests (McCaughey, 1985, 1987; Baldocchi *et al*., 2000). Coniferous species are more efficient in exchanging water and energy with the

* Correspondence to: M. A. Arain, School of Geography and Earth Sciences, McMaster University, 1280 Main Street West, Hamilton, ON, L8S 4K1, Canada. E-mail: arainm@mcmaster.ca

atmosphere as compared to deciduous species because of their distinct physiological and structural properties, e.g. stomatal control, roughness, conical architecture, needle clumping etc. Coniferous species have a lower albedo and absorb more radiation than deciduous species. Coniferous species also start to photosynthesize, and hence transpire water, early in the growing season while deciduous species are still dormant. Therefore, coexistence of both coniferous and deciduous species in the mixedwood forests creates unique environmental, hydrological and physiological conditions (McCaughey, 1985, 1987). Most past studies of energy, carbon dioxide and water vapour exchanges in the boreal region have focused on pure, single-species, forest stands (Blanken *et al*., 1997; Jarvis *et al*., 1997; Sellers *et al*., 1997; Baldocchi *et al*., 2001; Arain *et al*., 2002, 2003). Hence, our current understanding of surface-atmosphere exchanges in mixedwood forests is poor, and any effort to help increase our knowledge of these interactions is of great value. Baldocchi *et al*. (2000) and Watson *et al*. (2000) have further highlighted the importance of land surface-atmosphere interactions in natural and managed forest ecosystems for regional and global climate change studies.

In order to enhance our understanding of land surface-atmosphere interactions in mixedwood forests, in the summer of 2003 we initiated long-term year-round measurements of energy, carbon dioxide and water vapour fluxes in a 74-year-old boreal mixedwood forest in northern Ontario, Canada, known as the Groundhog River Flux Station (GRFS). The GRFS is part of the Fluxnet-Canada Research Network (FCRN) (Fluxnet-Canada, 2006), which is a national research network of flux towers from the east coast to the west coast of Canada and includes both forested and wetland ecosystems. In this paper, we present energy and water exchanges at the GRFS for the first year of measurements from 1 September 2003 to 31 August 2004. The main objectives of this paper are: (i) to describe diurnal and seasonal cycles of radiation, energy and water vapour fluxes and to estimate annual evapotranspiration, (ii) to discuss the role of canopy conductance in controlling the rate of evapotranspiration, and (iii) to characterize the major environmental controls on seasonal variations of water loss from this boreal mixedwood forest.

MATERIALS AND METHODS

Site description

The study site (48·217 °N and 82·156 °W) is located in a typical boreal mixedwood forest in northeastern Ontario, Canada, approximately 80 km southwest of Timmins, near the Groundhog River. This forest developed after high-grade logging in the 1930s. The forest is dominated by five species characteristic of Ontario mixedwoods: trembling aspen (*Populus tremuloides* (Michx.), black spruce (*Picea mariana* (Mill.) B.S.P.), white spruce (*Picea glauca* (Moench.) Voss.), white birch (*Betula papyrifera* Marsh.), and balsam fir (*Abies balsamea* (L.) Mill.). In some patches of the forest, eastern white cedar (*Thuja occidentalis* L.) can be found. The degree of spatial structure for the site was evaluated from a variety of sources and techniques, including remote sensing data and more traditional cruise line data collection. The cruise line analysis indicated that in the northwest, the species composition is equally (50 : 50) divided between coniferous and deciduous species. In the northeast, the deciduous to coniferous species ratio is 56 : 44, while in the southwest the distribution of species is 53 : 47. The southeast region has significantly more deciduous species where the ratio is 65 : 35. A more detailed analysis of the species distribution, based on remote sensing of total chlorophyll and biomass (pixel size 4×4 m), was used to delineate the major species and species groupings, and the results supported the contention that the site is mixed but is relatively homogeneous (McCaughey *et al*., 2006). With respect to the spatial distribution of individual species (white birch, black spruce, eastern cedar, and trembling aspen), the same conclusion was warranted. The canopy top height varies between 30 and 32 m, and the basal area of the sectors varies from 22 to 27 $m^2\ ha^{-1}$, except in the southwest region, which has a slightly lower value of 18·4 $m^2\ ha^{-1}$.

The forest has a rich understory of short herbaceous species and mosses (feather moss and sphagnum moss), and Lycopodium (club moss). The soil has a 15-cm-thick organic layer and a deep B-horizon. The latter is characterized as a silty, very fine sand that has a 25-cm-deep upper layer, tentatively identified as a Bf horizon, which overlies a deep lighter coloured layer. The B-horizon also contains boulders of varying sizes, ranging from a few centimetres in diameter to few tens of centimetres. In this forest, tree roots are shallow and mostly residing in the upper organic soil layer (Khomik *et al.*, 2006).

Flux and supplementary measurements

Eddy covariance (EC) flux instruments are installed at a height of 43·3 m on top of a 41-m high walk-up double scaffolding tower. The tower is located in the centre of a stand that is 2 km in diameter. Our analysis with a footprint model indicated that fetch extends to about 800 m during the day to a few kilometres during calm conditions at night. The same type of forest stretches for many kilometres in all directions. EC flux measurements and data analysis followed FCRN protocols (Fluxnet-Canada, 2006). Half-hourly fluxes of momentum, sensible heat (H), latent heat (LE) and carbon dioxide (CO_2) were measured using an open-path EC system from mid-July 2003 to October 2003, and then, starting in October 2003, these fluxes were measured using a closed-path EC system. Flux measurements have continued uninterrupted until the writing of this paper; however fluxes recorded after 31 August 2004 are not reported in this paper. The open-path EC system consisted of a three-dimensional sonic anemometer (model CSAT3, Campbell Scientific Inc. (CSI), Logan, Utah, USA), an infrared gas analyzer (IRGA) (model LI-7500, LI-COR, Lincoln, Nebraska, USA), and a fine-wire (12·5 μm in diameter) thermocouple located near the centre of the sonic array. The closed-path EC system consisted of a three-dimensional sonic anemometer (model CSAT3, CSI, Logan, Utah, USA) and an IRGA (model LI-7000, LI-COR, Lincoln, Nebraska, USA). The closed-path IRGA was housed in a temperature-controlled box on top of the tower and was used to measure CO_2 and water vapour concentrations (mixing ratios). Air was drawn through a 4-m-long insulated Synflex tube (4 mm inner diameter) into the sample cell using a pump at a rate of 10 L min^{-1}, resulting in sample cell pressures of about 10 kPa less than the atmospheric pressure. A 1 μm teflon filter was installed upstream from the closed-path IRGA to prevent contamination of the optical chamber. The inlet of the sample tube was located about 10–12 cm below the sonic array. The short tube length and high flow rates eliminated the need for frequency response corrections. To prevent condensation, the sampling tube was heated 7–8 °C above ambient temperature. In order to raise the temperature of the sampled air to that of the IRGA sample cell, the air, before entering the system, was passed through a 0·5-m-long coiled copper tube with an interior diameter of 3 mm, situated between aluminium plates. The heated Synflex and copper tubes eliminate fluctuations in the temperature of the airstream. The sample tube caused a delay time of about 0·8 s in the measurement of the H_2O and CO_2 concentrations from the time of collection. Subsequent comparison of our closed-path EC system with the FCRN cross-site roving EC system indicated that the differences between fluxes from the two EC systems were within 2%. Our analysis using closed-path EC flux data from January to July 2004 when all cross products were available, as well as the comparison with the FCRN cross-site roving EC system, indicated that coordinate rotation was not an issue (1–5% difference in 0-rotated and 3-rotated fluxes) for the GRFS site because of its almost flat terrain. Therefore, this correction was not applied during post processing of fluxes presented in this paper. The closed-path IRGA was operated in absolute mode with dry (CO_2- and H_2O-free) nitrogen gas continuously passing through its reference cell at 80–90 cm^3 min^{-1}. The IRGA was calibrated once per day with ultra-high purity nitrogen gas for the zero offset check and CO_2 gas (360 μmol mol^{-1} CO_2 in air, referenced to primary standards traceable to the World Meteorological Organization CO_2 standards) for the CO_2 span check. All flux data were recorded at 20 Hz with a data logger (model CR5000, CSI, Logan, Utah, USA). Half-hourly H, LE, and CO_2 fluxes were derived on-line, and were saved every few days, along with high frequency flux data, on a storage disk housed in an instrument hut near the tower. AC power was supplied at the site to operate all equipment. Before installation at the GRFS site, the open-path EC system was tested and compared with a similar closed-path EC system installed at a forested site in southern Ontario. This comparison showed that both systems gave similar results.

A set of supporting meteorological variables were measured, including air temperature (T_a) and relative humidity, wind speed and direction, net radiation (R_n) and its components, incoming and outgoing photosynthetic photon flux density (*PPFD*), diffuse photosynthetically active radiation (*PAR*), soil heat flux (G), soil

DOI: 10.1002/hyp

water content by volume (θ), and soil temperature (T_s) at several depths, atmospheric pressure, precipitation (P), and snow depth. T_a and relative humidity were measured with humidity and temperature probes (model HMP45C, CSI, Logan, Utah, USA) installed at 41, 21, 10 and 2 m. Above-canopy T_a was measured with a platinum resistance thermometer (PRT) (model RTD-810, Omega Engineering Inc. Laval, Quebec, Canada) in an aspirated shield (model 076B-1, MetOne Instruments Inc., Grants Pass, Oregon, USA). Wind direction and wind speed measurements were recorded at the top of the tower at 43·3 m with a propeller wind vane/anemometer (wind monitor, model 05103, R.M. Young, Traverse City, Michigan, USA). Wind speed was also measured at 21, 10 and 2 m with 3-cup anemometers (model 12102, R.M. Young, Traverse City, Michigan, USA).

Downwelling and upwelling shortwave and longwave radiation were measured with a four-way net radiometer (model CNR 1, Kipp and Zonen, Delft, Netherlands) mounted on a square boom that projected horizontally at a distance of 5 m to the south side of the tower at a height of 37 m. R_n was derived by algebraically adding the four separate radiation fluxes (positive for incoming and negative for outgoing). Below-canopy R_n was also measured at 2 m using a net radiometer (model NR LITE, Kipp and Zonen, Delft, Netherlands). Downwelling and upwelling *PPFD* (model LI-190, LI-COR, Lincoln, Nebraska, USA) and diffuse *PAR* (model BF2, Delta-T Devices, Cambridge, UK), were also measured at 37 m. Atmospheric pressure was recorded with a pressure sensor (model CS105, Vaisala Oyj, Helsinki, Finland). Soil measurements were made at two locations. At each location, T_s was measured at depths of 2, 5, 10, 20, 50 and 100 cm, with 24 a.w.g. (American Wire Gauge) thermocouples distributed along a wooden dowel, and θ was measured with water content reflectometers (model CS615, CSI, Logan, Utah, USA) at depths of 5, 10, 20 and 50 cm. G was measured with two soil heat flux plates (model HFT3, manufactured by Radiation and Energy Balance Systems (REBS)) at 10 cm below the surface. Values of G from all soil heat flux plates were averaged to give a site average value that was used in the analysis. Each soil measurement location was about 100 m from the base of the tower, one to the north and one to the west. Snow depth was measured with a sonic ranger (model SR50, CSI, Logan, Utah, USA) at the north location. Precipitation amount and rate were measured with a tipping bucket rain gauge (model CS700, CSI, Logan, Utah, USA) and an accumulating gauge (model T200X, Geonor, Oslo, Norway). Both gauges were located in an open area on the edge of the site, approximately 1·5 km from the tower. During the winter, data from the tipping bucket were not available. All meteorological and soil data were recorded at half-hour intervals with data loggers (models CR23X and CR7X, CSI, Logan, Utah, USA).

Data corrections and gap filling

The average flux data recovery during the 12-month experimental period was 85%, which is higher than the average flux recovery reported for many other EC flux sites (Baldocchi *et al*., 2001; Wilson *et al*., 2002). Water vapour and CO_2 fluxes from the open-path EC system were corrected for the effects of air density fluctuations (Webb *et al*., 1980). This correction is intrinsic in the closed-path IRGA because of mixing ratio measurements. Energy balance closure of measured fluxes was calculated by comparing the turbulent fluxes ($H + LE$) with the available energy (R_n-G-S), where S is the canopy heat storage (Figure 1). The slope of the regression line for half-hourly fluxes is 0·96, with an intercept of 17 W m^{-2} and correlation coefficient of 0·84. It should be noted that no corrections were applied to the flux data to close the forest energy balance. Although non-closure of the energy balance was reported by many authors (such as Aubinet *et al*., 2001) as a common feature of EC measurements in terrestrial ecosystems, the causes of this non-closure are not fully known. Possible contributing causes include the absence of a fully developed turbulent boundary layer during calm conditions at night, localized large turbulent structures, possibly a result of topographic variation of canopy top height, which could cause on-site advection, and potential differences between the tower-based local value of R_n and that over the full flux footprint (Scheupp *et al*., 1990; Baldocchi, 2003). Despite being a multi-species heterogeneous site, energy balance closure estimates at the GRFS are in agreement with those reported at many forest sites (Wilson *et al*., 2002).

All flux and meteorological data were quality-controlled. Data gaps, which resulted from either failure of the system and calibration down time or from changing the system from open-path to closed-path EC

DOI: 10.1002/hyp

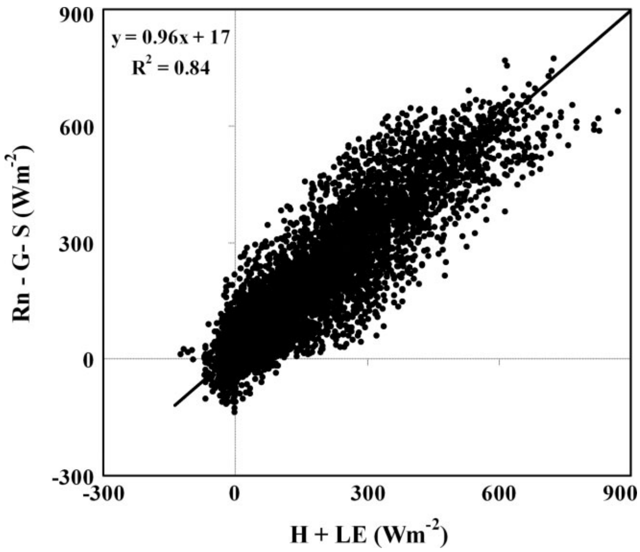

Figure 1. Half-hourly energy balance closure of the site. The net radiation minus soil heat flux and canopy heat storage (R_n-G-S) is plotted against the sum of sensible and latent heat fluxes ($H + LE$)

equipment, were filled using various methods depending on the nature and length of the gap. Small gaps (less than a few hours) were filled using linear interpolation. Longer gaps were filled by values derived from either mean diurnal ensemble values or with values from lookup tables (Falge *et al*., 2001). Gaps in P were filled using data from the closest weather station at Timmins airport, 80 km east of the site. For the month of December 2003, P data were missing, and the values measured at Timmins airport were inserted. During the experimental period, the prevailing wind direction at the GRFS varied from south through west to north, and, therefore, most of the measured fluxes shown in this paper originated from sectors that have almost a 50 : 50 ratio of deciduous and coniferous species (McCaughey *et al*., 2006).

RESULTS

Climatology of the site

Figure 2 shows the annual course of daily mean values of some of the key meteorological and soil variables for the study period. *PPFD* fluctuations clearly indicate frequent cloudy conditions through the year. The distribution of T_a also shows a large variation between winter and summer months, and its values ranged from $-30\,^{\circ}$C in January to about $+25\,^{\circ}$C in July. Radiation was at a maximum in June, while T_a reached its maximum in late July. There was a close coupling between T_s at 2 cm (T_s-2cm) and T_a trends. In winter, there was a large difference between T_a and T_s even at the 2-cm depth as a result of a thick snow cover that protected the ground from harsh winter temperatures. Daily mean vapour pressure deficit (*VPD*) during winter dropped to near zero and, during the growing season, the maximum daily mean values of *VPD* reached 1·7 kPa (Figure 5). In this forest, θ values were quite high because of the large P inputs and the high porosity of the organic layer that overlies the thick, lower, B-horizons at the site. Mean θ in the top 30-cm soil layer was about 0·43 m^3 m^{-3}. It ranged from 0·32 m^3 m^{-3} in late July and early August to 0·53 m^3 m^{-3} in April and May, following snowmelt. The total accumulated precipitation for the 12-month study period was 834 mm. The maximum daily rainfall of about 40 mm was recorded on 4 July 2004. The precipitation was distributed almost evenly over the year, except for lower levels in January and February. Large rainfall events generally occur in the summer and autumn months, and low precipitation in winter months is typical

DOI: 10.1002/hyp

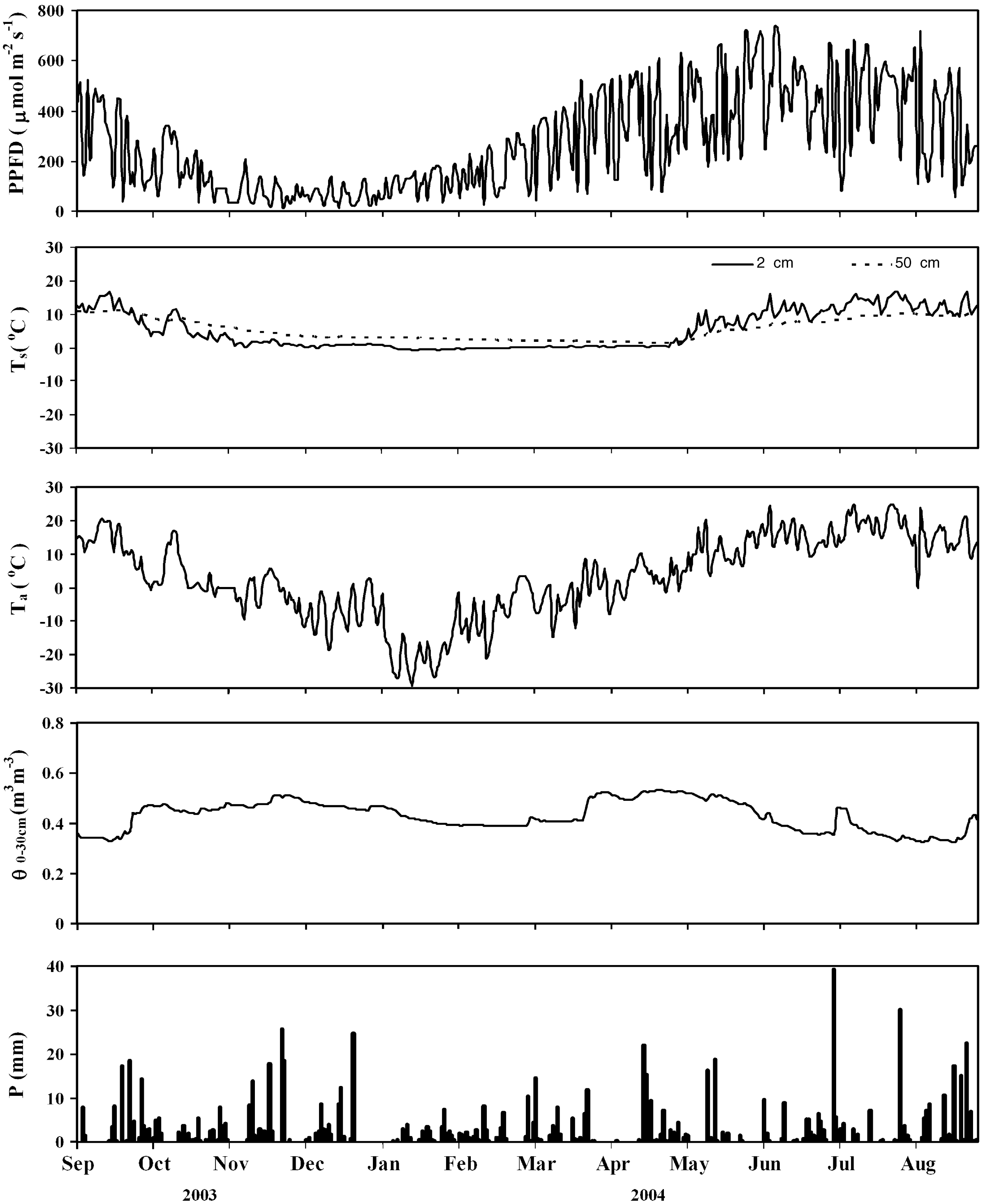

Figure 2. Annual course of daily mean values of meteorological variables at the site from 1 September 2003 to 31 August 2004, including *PPFD*, soil temperatures at 2 cm and 50 cm depths (T_s), air temperature (T_a), soil water content (θ) in 0–30 cm soil layer, and precipitation (P)

for southern boreal climates (McCaughey *et al.*, 1997). The site experienced surface run-off, lateral flow in the organic layer, and surface ponding in the spring and late autumn months.

Comparison of climatic conditions measured during the study period with climatic normals for the region indicated that mean monthly T_a at the site was 2 to 5 °C higher than normal in the summer of 2003 and winter of 2003–2004, except January 2004, which was approximately 4 °C colder than normal. In the spring and summer of 2004, the temperatures at the site were colder than normal by about 2 °C. The annual average T_a at GRFS for the study period was 2·1 °C higher than the annual normal T_a of 1·3 °C. This difference occurred mostly because of large positive anomalies in the winter months. The total annual precipitation (834 mm) was very close to the normal value of 831 mm. There were differences in snowfall at the GRFS site compared to the normal snowfall, with smaller amounts measured at the site in most winter months. This is consistent with the warmer winter experienced in the sample year. However, it is important to note that the spring snowmelt at the site was coincident with normal conditions, with April being the last month with significant snow accumulation.

Albedo

Albedo (the ratio of upward and downward shortwave radiation) has been cited as an important variable in global climate change modelling studies (Dickinson *et al.*, 1992; Betts and Ball, 1997; McCaughey *et al.*, 1997). Diurnal and seasonal patterns of albedo exert a strong influence on surface exchanges of heat and mass in terrestrial ecosystems, particularly in forests on both seasonal and annual timescales (McCaughey, 1987). Figure 3 shows the seasonal course of daily average albedo in this mixedwood forest. The distinct seasonal pattern of high and low albedo values is due to differences in phenology and spectral properties of the deciduous and coniferous species of this mixedwood stand. The daily albedo values ranged from about 0·07–0·09 in spring and fall months to about 0·15–0·17 in the winter months. Typical albedo values in the summer were about 0·12. Apart from some scatter because of varying atmospheric conditions, albedo remained almost constant (~0·12) throughout summer (June–September). A large scatter in winter albedo values (especially at the beginning of the dormant season) was a result of varying snow cover and depth on the forest floor, as well as frequent occurrences of snow-covered and non-snow-covered canopy states. Low albedo values observed in early spring and autumn were mostly due to high radiation absorption by the coniferous species, which amounted to 50% of stand density. Deciduous species that have higher canopy reflectance were leafless during this period. A similar phenomenon has been observed in other boreal forests (Betts, 2000; Claussen *et al.*, 2001; Betts and Ball, 1997; Arain *et al.*, 2003). Overall, summer albedo in this mixedwood forest was higher than values (<0·10) observed in pure coniferous forests. They were closer to values observed in the boreal deciduous forests which experience typical summer albedo values of 0·15–0·20 (Betts *et al.*, 2001).

Diurnal cycles of energy and water fluxes

Diurnal courses of 10-day mean energy fluxes for autumn (21–30 September 2003), winter (21–30 December 2003), spring (21–30 March 2004) and summer (21–30 June 2004) are shown in Figure 4. Corresponding diurnal courses of 10-day mean T_a and *VPD* are also shown. During autumn, R_n was low (<300 Wm^{-2}), and *LE* values were slightly higher than *H* because both T_a and R_n were high enough to support evapotranspiration (*E*) and photosynthetic activity. Peak mean *VPD* values were about 0·35 kPa, and atmospheric demand had not exerted any significant control on stomatal conductance. In winter, days were short, R_n was very low (<75 Wm^{-2}), T_a values were negative and *VPD* was close to zero. Winter $G + S$ values of about 20 Wm^{-2} were similar to *H* and *LE* values. In spring, although R_n increased significantly (>500 Wm^{-2}) both T_a and T_s were low and the forest was still dormant. *LE* values were <50 Wm^{-2} and most of the radiant energy was being transferred as sensible heat to the atmosphere (Figure 4). In summer, the forest started to grow and most of the energy was being partitioned as *LE* with its daytime peak values reaching up to 200 Wm^{-2}. T_a was more than 17 °C and *VPD* reached the highest point of the year with maximum

DOI: 10.1002/hyp

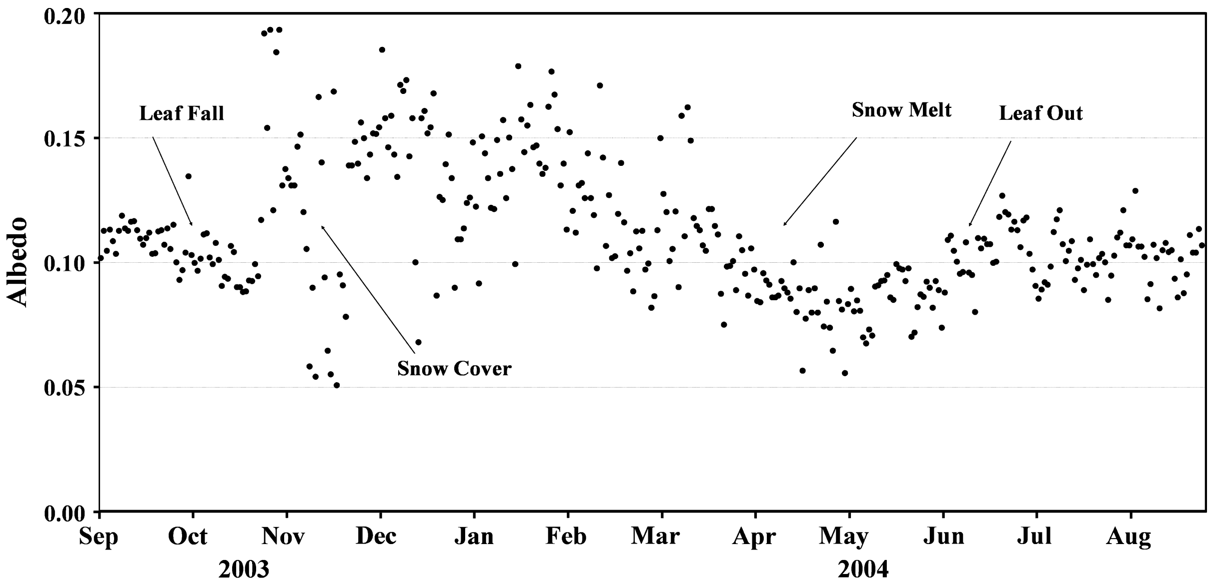

Figure 3. Variation of daily albedo during the experimental period (September 2003 to August 2004)

10-day mean values of 0·8 kPa. These *VPD* values were not high enough to initiate significant stomatal closure in response to high atmospheric demand in the afternoon hours. However, on some individual warm days in late summer (figure not shown) *VPD* values reached up to 1·7 kPa causing *LE* to decline during high atmospheric demand hours and making H a dominant turbulent flux (McNaughton and Black, 1973; Jarvis *et al*., 1997). In both autumn and summer seasons, small positive *LE* was observed even after sunset because of warm temperatures and high *VPD*.

Seasonal cycles of energy and water fluxes and evapotranspiration

The seasonal courses of mean daily values of R_n, H, *LE*, $G + S$ and *VPD* from September 2003 to August 2004 are illustrated in Figure 5. Apart from the typical seasonal trend, R_n showed large daily variations because of cloud cover and precipitation events. Pattey *et al*. (1997) and Arain *et al*. (2003) also reported the effect of afternoon cloudy conditions on energy and water exchanges in boreal ecosystems. The distribution of precipitation events throughout the year, and especially during the growing season, can explain most of the fluctuations in *LE* as well as in R_n and H. Maximum and minimum daily values of R_n ranged from -35 Wm^{-2} in winter to about 220 Wm^{-2} in summer. The seasonal course of H closely followed variations in R_n during the dormant season, but in the growing season *LE* also showed close correspondence with R_n. H remained the dominant flux from January through May. *LE* consistently increased through the spring (mid-April to May) as a result of the development of the deciduous canopy and increasing photosynthetic activity. June was the transition month, during which the energy partition balance shifted from H to *LE* as being the dominant convective flux. Daily mean *LE* or E reached its peak values in July, i.e. about 80–100 Wm^{-2} or 2–3 mm day^{-1} and remained high until late September, mostly because of the availability of abundant soil moisture. Occasionally, on warm and sunny days, daily E values exceeded their summer normal value and reached up to 4–5 mm day^{-1}. Maximum daily mean *VPD* values reached up to 1·7 kPa on some of the summer afternoons. During these high *VPD* hours, forest stomatal conductance, and hence evaporation, declined as a result of high atmospheric demand. June through September is considered the peak-growing season when a large portion of R_n is partitioned into *LE* in this mixedwood forest (Figure 5). In the summer and autumn seasons, *LE* remained positive for a few half-hours even after sunset; whereas the other energy components became slightly negative. This phenomenon was also observed in winter, but overall the values

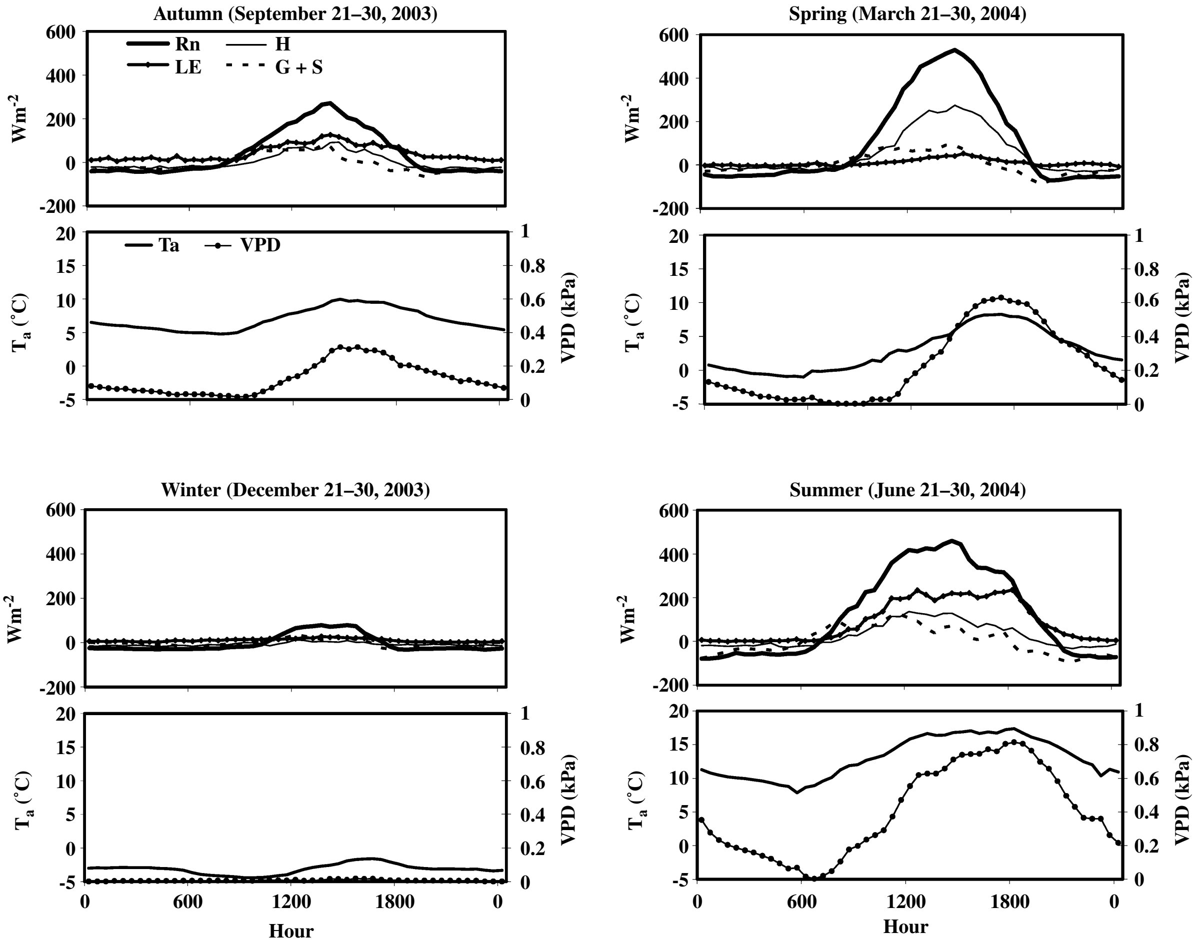

Figure 4. Diurnal course of ensemble net radiation (R_n), sensible heat flux (H), latent heat flux (LE), soil heat flux plus canopy heat storage ($G + S$), air temperature (T_a) and vapour pressure deficit (VPD) for a 10-day period in autumn, winter, spring and summer of 2003–2004

of evaporative flux were much smaller. Although the values of $G + S$ are much smaller than other fluxes, its day-to-day fluctuations followed variations in R_n. Daily values of G and S were comparatively small for most months, except from June to October.

In winter, T_s was close to zero, although T_a dropped to sub-zero values from December through March. In winter, all energy flux components were small and most of the available energy was partitioned as H, which closely followed the diurnal pattern of R_n. Over the same period, LE was low and T_s was close to zero. LE showed a weak association with R_n and always remained positive throughout winter because of a small amount of sublimation and evaporation during the warm hours of the day. Typical values of winter evaporation were 0·1 to 0·3 mm day^{-1} (Figure 5), similar to those reported for a boreal black spruce forest site (Arain *et al.*, 2003). No significant increase in LE was observed until mid-April when temperatures became positive and photosynthetic activity started in the coniferous species similar to past studies in boreal forests (Jarvis *et al.*, 1997; Baldocchi *et al.*, 2000; Arain *et al.*, 2003).

Figure 6 shows the time series of cumulative values of P, E and run-off plus infiltration (P-E), as well as the annual water balance of the forest. Daily total values of P are also shown. The total annual P from September 2003 to August 2004 was 835 mm, while the total amount of water loss as E during this period

DOI: 10.1002/hyp

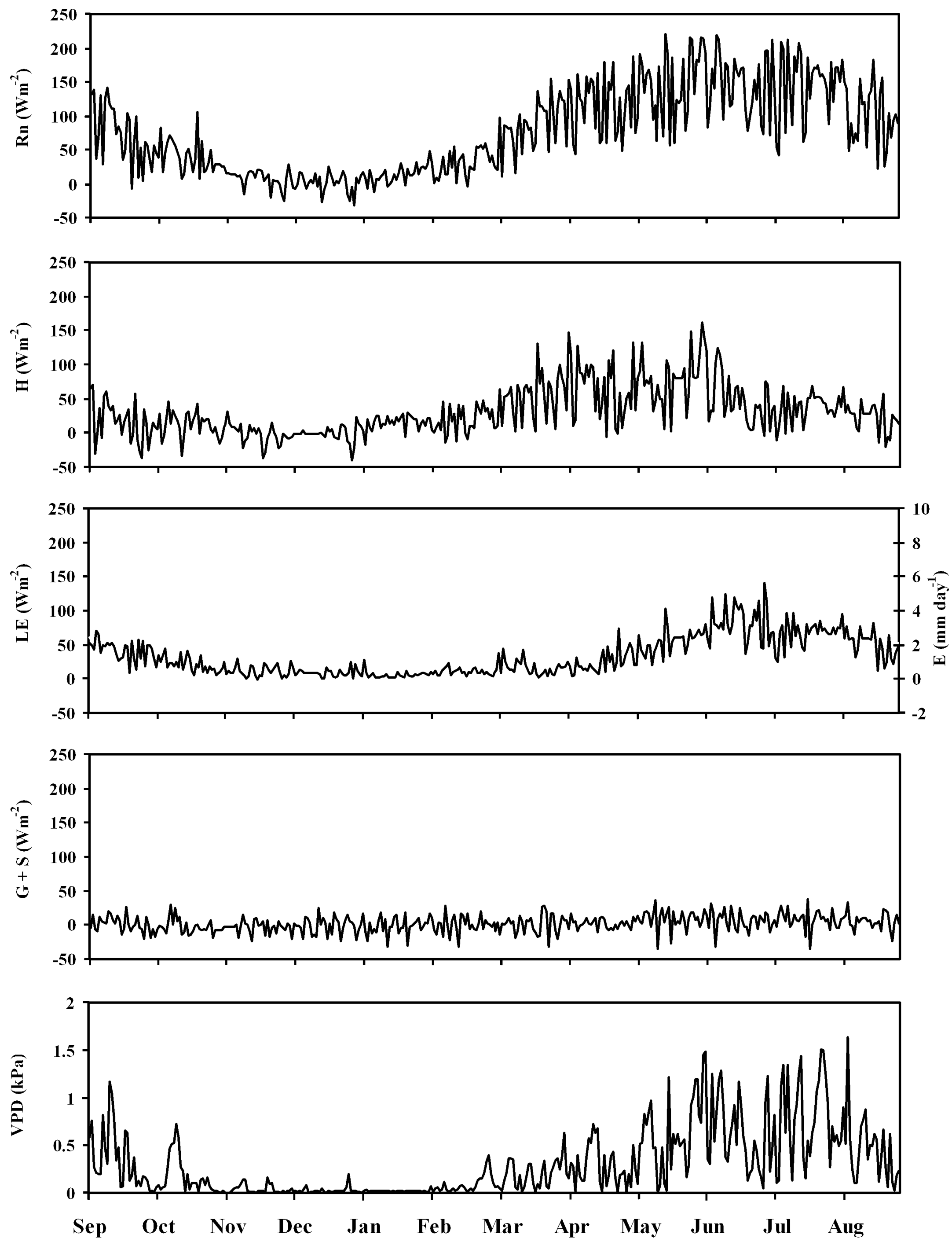

Figure 5. Seasonal course of daily mean net radiation (R_n), sensible heat flux (H), latent heat flux (LE), evapotranspiration (E), soil heat flux plus canopy heat storage ($G + S$) and vapour pressure deficit (VPD) from 1 September 2003 to 31 August 2004

DOI: 10.1002/hyp

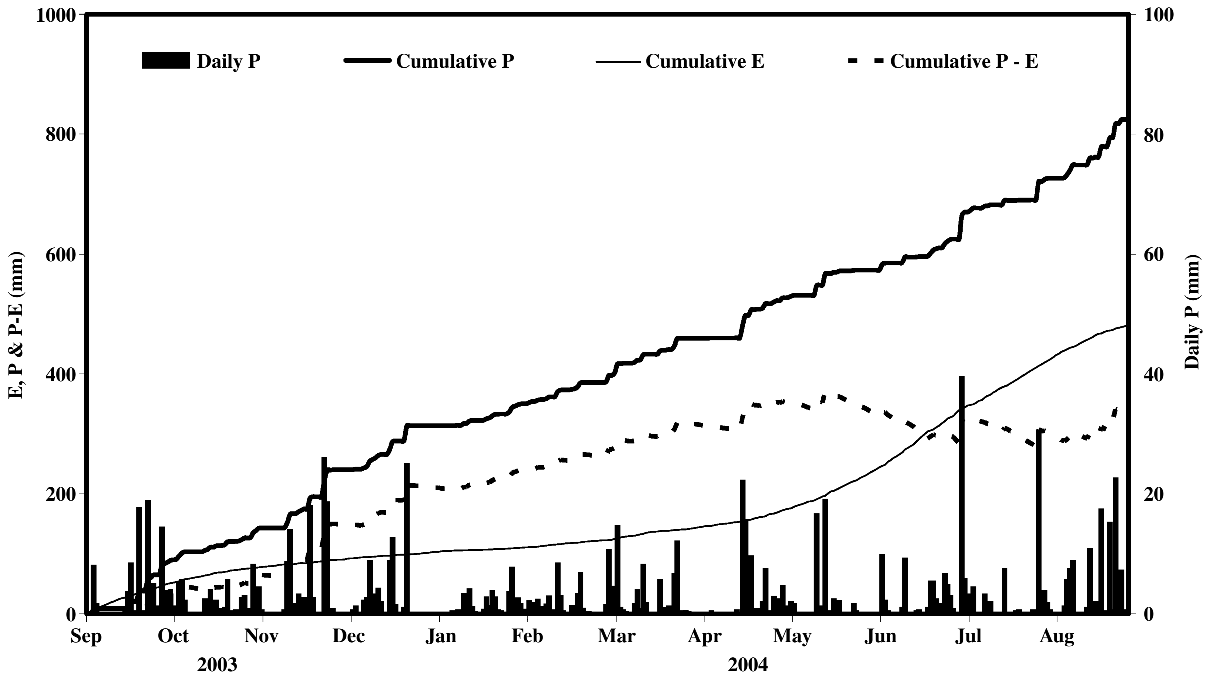

Figure 6. Cumulative precipitation (*P*), evapotranspiration (*E*), and precipitation minus evapotranspiration (*P-E*), as well as daily totals of *P*, from September 2003 to August 2004

was 480 ± 30 mm, which accounts for 57% of *P*. Most of the *E* occurred during the growing season, i.e. May through September. *P-E* indicated a rapid increase in April and May because of snowmelt and at the end of growing season in August and September when *E* started to decline because of diminishing atmospheric demand. In general, the trends in the rise and fall of (*P-E*) and soil water content values were consistent over the measurement period (Figures 2 and 5).

Surface conductance and its relationship to climatic factors and evapotranspiration

Bulk surface conductance to water vapour (G_S) was calculated from an inversion of the Penman–Monteith equation (Monteith, 1981; Blanken *et al.*, 1997). The Penman–Monteith equation provides a framework that includes the influence of available energy, atmospheric conditions (temperature, *VPD* and turbulence) and plant physiology (canopy conductance) on the water loss from vegetation. G_S is defined as the ratio of measured forest *LE* to the difference between the vapour pressure in the stomatal cavities (i.e. the saturation vapour pressure at canopy temperature) and the vapour pressure at the canopy surface. Typical half-hourly G_S values were about 4–15 mm s^{-1}, with maximum values reaching up to 48 mm s^{-1}. Similarly, typical daytime (when *PPFD* >200 μmol m^{-2} s^{-1} and the canopy was dry) mean G_S values were approximately 5–12 mm s^{-1}, with maximum values reaching up to 28 mm s^{-1} (Figure 7). These G_S values were higher than those reported for a boreal coniferous forest (Arain *et al.*, 2003) and quite comparable with values reported for a southern boreal deciduous forest (Blanken *et al.*, 1997; Barr *et al.*, 2001). Comparison of mean daytime G_S values with VPD for the rain-free periods showed a strong relationship during the growing season (Figure 7). There was an exponential decrease in G_S with the increase in *VPD*, indicating stomatal closure during high atmospheric demand and dry periods. This phenomenon has also been observed in other boreal forests during late afternoon hours (Hogg *et al.*, 2000) and during drought events (Baldocchi *et al.*, 2000). Figure 7 also shows some scatter between the G_S and *VPD* relationship for periods when atmospheric

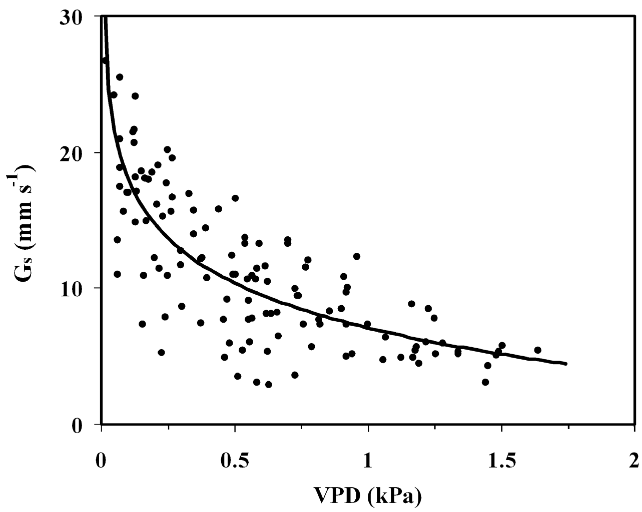

Figure 7. Relationship between daytime ($PPFD$ >200 µmol m^{-2} s^{-1}) mean surface conductance (G_S) and vapour pressure deficit (VPD) for the rain-free periods during the growing season (June–September) of 2004

demand was low (VPD < 0·8 kPa), indicating the influence of environmental factors on G_S (Law *et al.*, 2002).

In order to understand better the behaviour of evapotranspiration from the ecosystem and to characterize the forest evapotranspiration, the Priestley–Taylor α, defined as the ratio of measured LE to equilibrium LE [i.e. $LEeq = \frac{s}{s+\gamma}(R_n - G - S)$, where s is the change in saturation vapour pressure with T_a, and γ is the psychrometric constant], was calculated and compared with G_S (Priestley and Taylor, 1972). Priestley–Taylor's α provides a convenient way to estimate forest evapotranspiration. Other methods (e.g. Penman–Monteith equation) used for this purpose require many environmental and physiological parameters that are difficult to measure and often not available. Priestley–Taylor's α is also used to describe the regional interaction between the surface and the boundary layer (Blanken *et al.*, 1997). When α is greater than or close to unity, E is largely limited by energy availability and the water supply is unrestricted, whereas when α is less than unity, water limitations reduce E below the equilibrium evaporation rate.

Figure 8 shows the relationship between half-hourly daytime α values (when $PPFD$ >200 µmol m^{-2} s^{-1}) and G_S when the canopy was dry over the growing season. Large seasonal variations in G_S resulted in a wide range in α values despite high soil water content. It also shows that α is relatively insensitive to changes in G_S for the values larger than approximately 18–20 mm s^{-1}. Values of α observed in this mixedwood forest (especially during the full-leaf period) were almost twice the values recorded in a boreal coniferous forest (black spruce; Arain *et al.*, 2003), while they were slightly higher than or similar to values measured in a boreal deciduous forest (aspen; Blanken *et al.*, 1997). These results indicate that dry or water stress events were not common in this mixedwood forest. This is also evident by the high soil water content as shown in Figure 2. The analysis of α and G_S further indicated that this mixedwood forest is more similar to boreal deciduous stands in term of evapotranspiration, rather than boreal coniferous forests. Hence, a greater proportion of deciduous tree species in mixedwood stands may have a significant influence on energy and water exchanges in mixedwood forests. Because a large portion of the landscape in northern Ontario is occupied by mixedwood forests, understanding the evapotranspiration processes from these mixed stands will have important implications for regional water and carbon cycles.

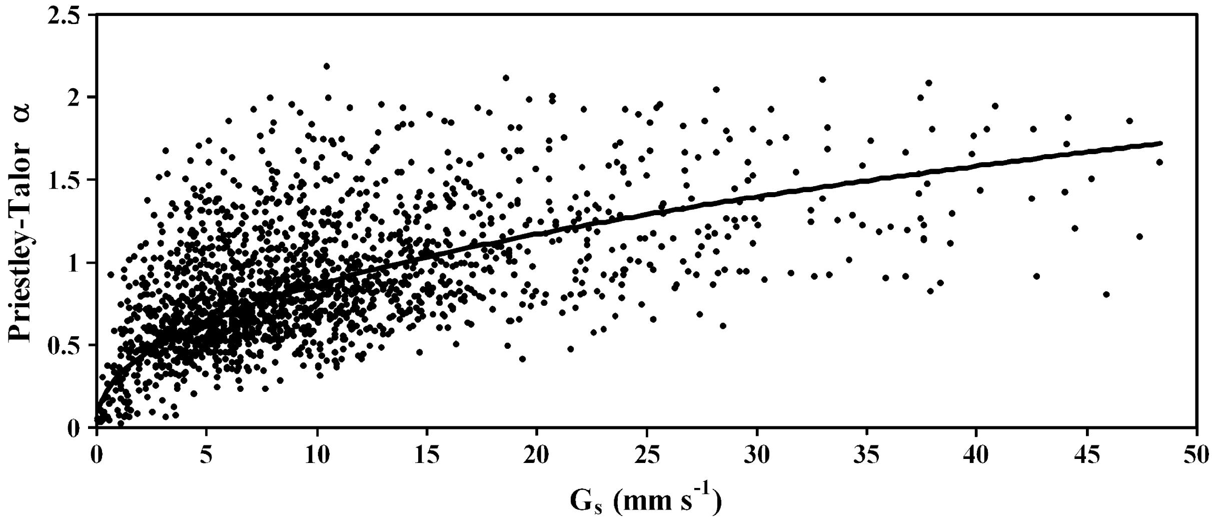

Figure 8. The relationship between half-hourly daytime (*PPFD* >200 µmol m^{-2} s^{-1}) Priestley–Taylor α values and surface conductance (G_S) for the rain-free periods during the growing season (June–September) of 2004

DISCUSSION

The distinct pattern of rise and fall in albedo observed in this boreal mixedwood forest shows varying controls of coniferous and deciduous species on the radiation and energy partitioning regimes. In general, summer albedo values observed in this forest (~0·12) were higher than those observed in pure coniferous stands (<0·10) and lower than those observed in pure deciduous forests (~0·15 to 0·20) (Betts *et al.*, 2001). Winter albedo values were typical of boreal forests reported in the literature. The largest change in albedo was observed in the spring and autumn shoulder seasons. These results have significance for radiation schemes incorporated in the land-surface interaction models used in global climate models (Kucharik *et al.*, 2000; Arain *et al.*, 2002). This study highlights the need to be cautious about seasonal dynamics of albedo, while parameterizing radiation and energy partitioning for mixed or heterogeneous forests. These results also indicate that detailed studies of the seasonal variation in albedo in mixedwood forests may provide quantitative information on surface heating to guide us in carefully selecting a mix of coniferous and deciduous plantation species and management approaches to mitigate climate warming through forest plantations.

Daily mean evaporation values of 2 to 3 mm day^{-1} during the growing season were comparable to values reported for other Canadian boreal forests (Black *et al.*, 1996; Blanken *et al.*, 1997; Lafleur, 1997; Arain *et al.*, 2003). These values were much higher than the average growing season values for most European boreal coniferous forests, which range from 1·4 to 2·1 mm day^{-1} (Kelliher *et al.*, 1997; Grelle *et al.*, 1999). However, average evaporation was greater in a boreal pine forest in Sweden: 3·4 mm day^{-1} (Lindroth, 1985). Similarly, the daily peak values of evaporation for the growing season were less than those for deciduous forests (e.g. maximum 6 mm day^{-1} reported by Black *et al.*, 1996) and, as expected, higher than coniferous forests (e.g. maximum 3·5 mm day^{-1} reported by Arain *et al.*, 2003). Frequent precipitation events throughout the year, and particularly in the growing season, kept soil water content high during 2003–2004. Winter evaporation values of 0·1 to 0·3 mm day^{-1} were similar to winter values observed in a boreal aspen forest (Black *et al.*, 1996) and a boreal mixed Norway spruce–Scots pine forest (Grelle *et al.*, 1999). The negative feedback between *VPD* and bulk surface conductance under water stress conditions limited evaporation mostly during the late summer periods. The seasonal course of Priestley–Taylor α values varied greatly from the typical 1·26 suggested for wet regions (Priestley and Taylor, 1972). As a result, extreme care is necessary when simple radiation-based models are used to estimate seasonal and annual evaporation in forest ecosystems.

DOI: 10.1002/hyp

The annual evaporation in this forest (480 mm $year^{-1}$) is high compared to other boreal forests. For example, Arain *et al*. (2003) reported 366 and 345 mm for a boreal black spruce forest in Saskatchewan, Canada in 1999–2000 and 2000–2001, respectively. Similarly, the annual evaporation from a boreal deciduous (aspen) stand at Prince Albert, Saskatchewan Canada was about 403 mm, which was 88% of annual precipitation (Black *et al*., 1996). The annual total evaporation from this mixedwood forest is closer to that observed in the boreal deciduous forests, rather than coniferous stands, although deciduous forests experience a shorter transpiration period than coniferous stands (Baldocchi *et al*., 2000). It seems that, despite having a short growing season, the presence of deciduous species causes higher evaporation in a mixedwood forest ecosystem.

As mentioned earlier, the influences of available energy, VPD, G_S, P and θ are important factors controlling the seasonal dynamics of evaporation from this mixedwood forest. Most of the roots in this forest are confined to the upper organic soil layer (Khomik *et al*., 2006); therefore, any changes in precipitation and soil moisture as a result of climate change will have an adverse impact on the growth of this forest. Various future climate predictions suggest increased frequency of extreme precipitation events in most regions, but relatively smaller increases in annual totals (McGuffie *et al*., 1999; New *et al*., 2001). Larger precipitation events would contribute more to surface run-off than to soil water storage. Depletion of soil water content would suppress intense growth and hence water loss from forest ecosystems during the short growing season. Changes in evaporation from these mixedwood forest ecosystems might also feed back on energy partitioning and boundary layer processes at regional scales (Baldocchi *et al*., 2000; Raupach, 1998).

CONCLUSIONS

In this paper, we report on energy and water vapour fluxes for the first year of a newly initiated flux tower site in a mixedwood boreal forest in northern Ontario, Canada. The principal findings are:

- The total annual precipitation from September 2003 to August 2004 was 835 mm, while the total amount of water loss (evapotranspiration) during this period was 480 ± 30 mm, which accounts for 57% of precipitation.
- Daily mean evapotranspiration values during the peak growing season were about 2 to 3 mm day^{-1} with maximum evapotranspiration values reaching up to 4 to 5 mm day^{-1} on sunny days with high atmospheric demand and turbulence.
- The seasonal pattern of daily albedo showed a distinct pattern in this mixedwood forest with the first low radiation reflection period in spring (between the time of snow melting and deciduous leaf-out) and the second low reflection period in autumn (just after senescence and before snowfall). These low albedo periods are attributed to the dominant influence of coniferous species in the spring and autumn seasons.
- Bulk surface conductance declined with increasing VPD indicating stomatal closure during high atmospheric demand and occasional dry periods. Bulk surface conductance values were relatively higher than those for other boreal coniferous forests and were closer to values typical of southern boreal deciduous forests.
- Priestley–Taylor α values during the growing season showed a wide range, but most of the time they were close to unity, indicating that for this forest ecosystem energy supply was the dominant control on evapotranspiration and that water was not a limiting factor.

ACKNOWLEDGEMENTS

Funding for this study was provided by the Natural Sciences and Engineering Research Council (NSERC) of Canada, the Canadian Foundation for Climate and Atmospheric Sciences (CFCAS), and the BIOCAP Canada Foundation through the Fluxnet-Canada Research Network (FCRN). Funding and support from the Canada

Foundation for Innovation, the Ontario Innovation Trust, Queen's University and McMaster University are also acknowledged. In-kind support from the Canadian Forest Service and Environment Canada is appreciated. We are grateful for assistance from Al Cameron (CFS), Daniel Finch, Don Zuiker, Reesa Dexter, Lauren MacLean, Myroslava Khomik, Elizabeth Wells, Kathryn Lundy and Rose Blair. The first author was supported by a graduate research assistantship from FCRN.

REFERENCES

Arain MA, Black TA, Barr AG, Morgenstern K, Nesic Z. 2003. Year-round observations of the energy and water vapour fluxes above a boreal black spruce forest. *Hydrological Processes* **17**: 3581–3600.

Arain MA, Black TA, Barr AG, Jarvis PG, Massheder JM, Verseghy DL, Nesic Z. 2002. Effects of seasonal and interannual climate variability on net ecosystem productivity of boreal deciduous and conifer forests. *Canadian Journal of Forest Research* **32**: 878–891.

Aubinet M, Chermanne B, Vandenhaute M, Longdoz B, Yernaux M, Laitat E. 2001. Long-term carbon dioxide exchange above a mixed forest in the Belgian Ardennes. *Agricultural and Forest Meteorology* **108**: 293–315.

Baldocchi DD. 2003. Assessing the eddy covariance technique for evaluating carbon dioxide exchange rates of ecosystems: past, present and future. *Global Change Biology* **9**: 479–492.

Baldocchi D, Falge E, Gu LH, Olson R, Hollinger D, Running S, Anthoni P, Bernhofer C, Davis K, Evans R, Fuentes J, Goldstein A, Katul G, Law B, Lee XH, Malhi Y, Meyers T, Munger W, Oechel W, U K, Pilegaard K, Schmid HP, Valentini R, Verma S, Vesala T, Wilson K, Wofsy S. 2001. Fluxnet: a new tool to study the temporal and spatial variability of ecosystem-scale carbon dioxide, water vapour and energy flux densities. *Bulletin of the American Meteorological Society* **82**: 2415–2434.

Baldocchi D, Kelliher FM, Black TA, Jarvis PJ. 2000. Climate and vegetation controls on boreal zone energy exchange. *Global Change Biology* **6**: 69–83.

Barr AG, Bett AK, Black TA, McCaughey JH, Smith CD. 2001. Intercomparison of BOREAS northern and southern study area surface fluxes in 1994. *Journal of Geophysical Research* **106**: 33543–33550.

Betts RA. 2000. Offset of the potential carbon sink from boreal forestation by decreases in surface albedo. *Nature* **408**: 187–190.

Betts AK, Ball JH. 1997. Albedo over the boreal forest. *Journal of Geophysical Research* **102**: 28901–28909.

Betts AK, Ball JH, McCaughey JH. 2001. Near-surface climate in the boreal forest. *Journal of Geophysical Research* **106**: 33529–33541.

Black TA, den Hartog G, Neumann HH, Blanken PD, Yang PC, Russell C, Nesic Z, Lee X, Chen SG, Staebler R, Novak MD. 1996. Annual cycles of water vapour and carbon dioxide fluxes in and above a boreal aspen forest. *Global Change Biology* **2**: 219–229.

Blanken PD, Black TA, Yang PC, den Hartog G, Neumann HH, Nesic Z, Novak MD, Staebler R, Lee X. 1997. Energy balance and surface conductance of a boreal aspen forest: partitioning overstory and understory components. *Journal of Geophysical Research* **102**: 28915–28927.

Claussen M, Brovkin V, Ganopolski A. 2001. Biogeophysical versus biogeochemical feedbacks of large-scale land cover change. *Geophysical Research Letters* **28**: 1011–1014.

Dickinson RE. 1992. Land Surface. In *Climate System Modelling*, Trenberth KE (ed.). Cambridge University Presss: Cambridge, 35–65.

Falge E, Baldocchi D, Olsam RJ, Anthoni P, Aubinet M, Bernhofer C, Burba G, Ceulemans R, Clement R, Dolman H, Granier A, Gross P, Grunwald T, Hollinger D, Jensen N, Katul G, Keronen P, Kowalski A, Lai CT, Law BE, Meyers T, Moncrieff J, Moors E, Munger W, Pielegaard K, Rannik U, Rebmann C, Suyker A, Tenhunen J, Tu K, Verma S, Vesals T, Wilson K, Wofsy S. 2001. Gap filling strategies for defensible annual sums of net ecosystem exchange. *Agricultural and Forest Meteorology* **107**: 43–69.

Fluxnet-Canada. Website 2006. http://www.fluxnet-canada.ca.

Grelle A, Lindroth A, Mölder M. 1999. Seasonal variation of boreal forest surface conductance and evaporation. *Agricultural and Forest Meteorology* **98–99**: 563–578.

Hogg EH, Saugier B, Pontailler J-Y, Black TA, Chen W, Hurdle PA, Wu A. 2000. Responses of trembling aspen and hazelnut to vapour pressure deficit in a boreal deciduous forest. *Tree Physiology* **20**: 725–734.

Jarvis PG, Massheder JM, Hale SE, Moncrieff JB, Rayment M, Scott SL. 1997. Seasonal variation of carbon dioxide, water and energy exchanges of a boreal black spruce forest. *Journal of Geophysical Research* **102**: 28953–28966.

Kelliher FM, Hollinger DY, Schulze E-D, Vygodskaya NN, Byers JN, Hunt JE, McSeveny TM, Milukova I, Sogatchev A, Varlargin A, Ziegler W, Arneth A, Bauer G. 1997. Evaporation from an eastern Siberian larch forest. *Agricultural and Forest Meteorology* **85**: 135–147.

Khomik M, Arain MA, McCaughey JH. 2006. Temporal and spatial variability of soil respiration in a boreal mixedwood forest. *Agricultural and Forest Meteorology* (in press).

Kucharik CJ, Foley JA, Delire C, Fisher VA, Coe MT, Lenters JD, Young-Molling C, Ramankutty N. 2000. Testing the performance of a dynamic global ecosystem model: water balance, carbon balance, and vegetation structure. *Global Biogeochemical Cycles* **14**: 795–825.

Lafleur P. 1997. Energy balance and evapotranspiration from a subarctic forest. *Agricultural and Forest Meteorology* **58**: 163–175.

Law BE, Falge E, Gu L, Baldocchi DD, Bakwin P, Berbigier P, Davis K, Dolman AJ, Falk M, Fuentes JD, Goldstein A, Granier A, Grelle A, Hollinger D, Janssenss IA, Jarvis P, Jensen NO, Katul G, Mahli Y, Matteucci G, Meyers T, Monson R, Munger W, Oechel W, Olson R, Pilegaard K, Paw UKT, Thorqeirsson H, Valentini R, Verma S, Vesala T, Wilson K, Wofsv S. 2002. Environmental controls over carbon dioxide and water vapour exchange of terrestrial vegetation. *Agricultural and Forest Meteorology* **113**: 97–120.

Lindroth A. 1985. Seasonal and diurnal variation of energy budget components in coniferous forests. *Journal of Hydrology* **82**: 1–15.

McCaughey JH. 1985. Energy balance storage terms in a mature mixed forest at Petawawa, Ontario_a case study. *Boundary-Layer Meteorology* **31**: 89–101.

McCaughey JH. 1987. The albedo of a mature mixed forest and a clearcut site at Petawawa, Ontario. *Agricultural and Forest Meteorology* **40**: 251–263.

DOI: 10.1002/hyp

McCaughey JH, Pejam MR, Arain MA, Cameron A. 2006. Carbon balance of a boreal mixedwood forest ecosystem in Ontario, Canada. *Agricultural and Forest Meteorology* (in press).
McCaughey JH, Lafleur PM, Joiner DW, Bartlett PA, Costello AM, Jelinski DE, Ryan MG. 1997. Magnitudes and seasonal patterns of energy, water and carbon exchanges at a boreal young jack pine forest in the BOREAS northern study area. *Journal of Geophysical Research* **102**: 28997–29007.
McNaughton KG, Black TA. 1973. A study of evapotranspiration from Douglas fir forest using the energy balance approach. *Water Resources Research* **9**: 1579–1590.
McGuffie K, Henderson-Sellers A, Holbrook N, Kothavala K, Balachova O, Hoekstra J. 1999. Assessing simulations of daily temperature and precipitation variability with global climate models for present and enhanced greenhouse climates. *International Journal of Climatology* **19**: 1–26.
Monteith JL. 1981. Evaporation and surface temperature. *Quarterly Journal of the Royal Meteorological Society* **107**: 1–27.
New M, Todd M, Hulme M, Jones P. 2001. Precipitation measurements and trends in the twentieth century. *International Journal of Climatology* **21**: 1889–1922.
Pattey E, Desjardin RL, St-Amour G. 1997. Mass and energy exchange over a black spruce forest during key periods of BOREAS 1994. *Journal of Geophysical Research* **102**: 28967–28975.
Priestley CHB, Taylor RJ. 1972. On the assessment of surface heat flux and evaporation using large scale parameters. *Monthly Weather Review* **100**: 81–92.
Raupach MR. 1998. Influence of local feedbacks on land-air exchange of energy and carbon. *Global Change Biology* **4**: 477–494.
Scheupp PH, Leclerc MY, MacPherson JI, Desjardins RL. 1990. Footprint prediction of scalar fluxes from analytical solutions to the diffusion equation. *Boundary-Layer Meteorology* **50**: 355–373.
Sellers PJ, Hall FG, Kelly RD, Black TA, Baldocchi DD, Berry J, Ryan M, Ranson KJ, Crill PM, Lettenmaier DP, Margolis H, Cihlar J, Newcomer J, Fitzjarrald D, Jarvis PG, Gower ST, Halliwell D, Williams D, Goodison B, Wickland DE, Guertin FE. 1997. BOREAS in 1997: Experiment overview, scientific results and future directions. *Journal of Geophysical Research* **102**: 28731–28770.
Watson RT, Noble IR, Bolin B, Ravindranath NH, Veraado DJ, Drokken DJ. 2000. *Land Use, Land-Use Change and Forestry. A Special Report of the International Panel on Climate Change*. Cambridge University Press: Cambridge.
Webb EK, Pearman GI, Leunning R. 1980. Correction of flux measurements for density effects due to heat and water vapour transfer. *Quarterly Journal of the Royal Meteorological Society* **106**: 85–100.
Wilson K, Goldstein A, Falge E, Aubinet M, Baldocchi D, Berbigier P, Bernhofer C, Ceulemans R, Dolman H, Field C, Grelle A, Ibrom A, Law BE, Kowalski A, Meyers T, Moncrieff J, Monson R, Oechel W, Tenhunen J, Valentini R, Verma S. 2002. Energy balance closure at FLUXNET sites. *Agricultural and Forest Meteorology* **113**: 223–243.